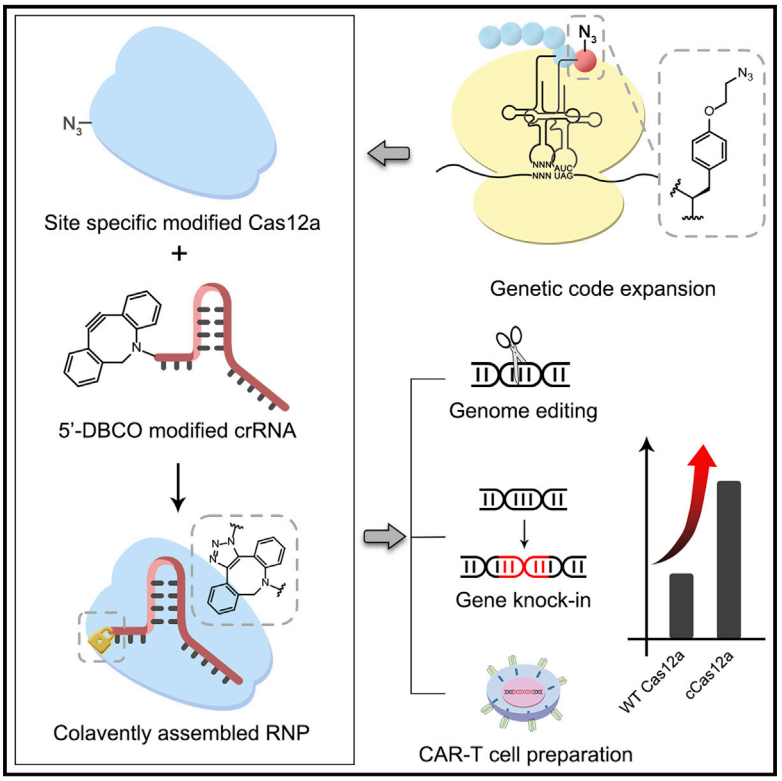
Molecular Cell



# Improving the efficiency of CRISPR-Cas12a-based genome editing with site-specific covalent Cas12a-crRNA conjugates

## Graphical abstract




## Highlights

- Site-specific modification of Cas12a using noncanonical amino acid mutagenesis
- Preparation of a covalent Cas12a-crRNA complex using bio-orthogonal chemistry
- Cas12a-crRNA conjugates increase genome editing efficiency
- Cas12a-crRNA conjugates afford site-specific CAR-T preparation with high efficiency

## Authors

Xinyu Ling, Liying Chang, Heqi Chen, ..., Bo Zhang, Jiazhi Hu, Tao Liu

## Correspondence

taoliupku@pku.edu.cn

## In brief

Ling et al. report a method to produce a covalently conjugated Cas12a-crRNA complex using bio-orthogonal chemistry with a site-specifically modified Cas12a protein and a 5′ chemically modified crRNA. The covalent ribonucleoprotein increases Cas12a genome editing efficiency and enables efficient multiplex genome editing in a CAR-T cell preparation.

Ling et al., 2021, Molecular Cell *81*, 4747–4756
November 18, 2021 © 2021 Elsevier Inc.
https://doi.org/10.1016/j.molcel.2021.09.021

CellPress

Molecular Cell

CellPress

Technology

# Improving the efficiency of CRISPR-Cas12a-based genome editing with site-specific covalent Cas12a-crRNA conjugates

Xinyu Ling,[1,5] Liying Chang,[1,5] Heqi Chen,[1] Xiaoqin Gao,[1] Jianhang Yin,[2,3] Yi Zuo,[1] Yujia Huang,[1] Bo Zhang,[4] Jiazhi Hu,[2,3] and Tao Liu[1,6,*]

[1]State Key Laboratory of Natural and Biomimetic Drugs, School of Pharmaceutical Sciences, Peking University, 38 Xueyuan Road, Haidian District, Beijing 100191, China

[2]The MOE Key Laboratory of Cell Proliferation and Differentiation, Genome Editing Research Center, School of Life Sciences, Peking University, Beijing 100871, China

[3]Peking-Tsinghua Center for Life Sciences, Peking University, Beijing 100871, China

[4]Department of Medical Research Center, Peking Union Medical College Hospital, Chinese Academy of Medical Sciences and Peking Union Medical College, Beijing 100730, China

[5]These authors contributed equally

[6]Lead contact

*Correspondence: taoliupku@pku.edu.cn

https://doi.org/10.1016/j.molcel.2021.09.021

## SUMMARY

The CRISPR-Cas12a system shows unique features compared with widely used Cas9, making it an attractive and potentially more precise alternative. However, the adoption of this system has been hindered by its relatively low editing efficiency. Guided by physical chemical principles, we covalently conjugated 5′ terminal modified CRISPR RNA (crRNA) to a site-specifically modified Cas12a through biorthogonal chemical reaction. The genome editing efficiency of the resulting conjugated Cas12a complex (cCas12a) was substantially higher than that of the wild-type complex. We also demonstrated that cCas12a could be used for precise gene knockin and multiplex gene editing in a chimeric antigen receptor T cell preparation with efficiency much higher than that of the wild-type system. Overall, our findings indicate that covalently linking Cas nuclease and crRNA is an effective approach to improve the Cas12a-based genome editing system and could potentially provide an insight into engineering other Cas family members with low efficiency as well.

## INTRODUCTION

CRISPR-Cas systems are widely used for genome editing and gene regulation in human cells and those of other organisms (Hsu et al., 2014; Wright et al., 2016; Dominguez et al., 2016; Anzalone et al., 2020). The DNA cleavage complex of these systems is composed of a Cas nuclease and a CRISPR RNA (crRNA). In addition to the most commonly used nuclease, *Streptococcus pyogenes* Cas9, some additional family members have been identified (Wang et al., 2016; Nakade et al., 2017). For example, Cas12a is an RNA-guided class II nuclease with some attractive features that are distinct from those of Cas9: (1) Cas12a recognizes specific thymine (T)-rich protospacer adjacent motif sequences (TTTN) that differ from the sequence recognized by *S. pyogenes* Cas9 (NGG) (Zetsche et al., 2015), and (2) the incidence of off-target effects with Cas12a is much lower than that with Cas9, which makes Cas12a a potentially safer choice for clinical applications (Kim et al., 2015; Tsai et al., 2015; Kleinstiver et al., 2016). Despite these advantages, the CRISPR-Cas12a system has not been adopted as readily as expected for the past several years. One of the key limitations in applying Cas12a is its relatively low efficiency for human genome editing (Bin Moon et al., 2018). Several methods have been applied to improve Cas12a-based genome editing efficiency in mammalian cells through protein engineering (Kleinstiver et al., 2019; Liu et al., 2019; Jones et al., 2021) or RNA engineering (Li et al., 2017; Bin Moon et al., 2018; Kocak et al., 2019). Whereas Cas9 binds either with two RNAs (crRNA and *trans*-activating crRNA) or with an approximately 100 nt single guide RNA, Cas12a relies entirely on one much shorter crRNA (~42 nt). The reported binding affinities between Cas12a and crRNA vary from a few nanomolar to a few dozen nanomolar (Dong et al., 2016; Bin Moon et al., 2018), a range that is 3–4 orders of magnitude lower than that reported for Cas9 and single guide RNA ($K_d$ = 10 pM) (Wright et al., 2015). We speculated that the low editing efficiency of Cas12a in mammalian cells could be attributed at least partially to the relatively weak interaction between the Cas protein and the crRNA.

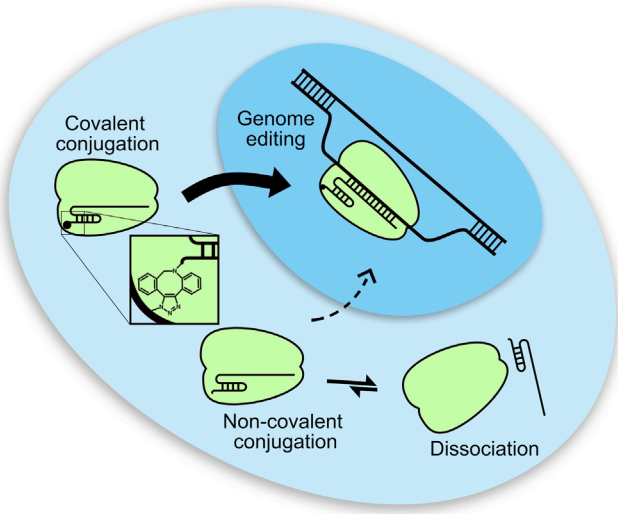



**Figure 1. Conversion of a three-component DNA cleavage reaction to a two-component one by means of site-specific biorthogonal conjugation**

## Design

We envisioned that the weak interaction of Cas12a nuclease and crRNA could be circumvented by covalently conjugating the two components into a single unit. To explore this possibility, we generated a Cas12a protein that was site-specifically modified with an azido group by means of noncanonical amino acid mutagenesis via an expanded genetic code (Liu and Schultz, 2010; Dumas et al., 2015; Chin, 2017; Ling et al., 2020a). The resulting protein mutant was covalently conjugated with crRNA modified at the 5′ terminus with dibenzocyclooctyne (DBCO) through a strain-promoted alkyne-azide cycloaddition reaction (Rostovtsev et al., 2002; Agard et al., 2004) to generate an active ribonucleoprotein (RNP). In this way, we could convert a three-component DNA cleavage reaction into a two-component reaction. The RNP could be delivered directly into cells, which is now considered to be the safest and most accurate for therapeutic applications.(Zuris et al., 2015) The covalent linkage could prevent the complex dissociation before RNP reaching the target loci (Figure 1). Indeed, we demonstrated that in mammalian cells, the cCas12a system displayed substantially higher genome editing efficiency than wild-type (WT) system. To demonstrate the utility of this strategy, we showed that the cCas12a platform could be applied to precise genome knockin and multiplex gene editing for chimeric antigen receptor T cell (CAR-T) preparation with higher efficiency than that of the WT system, making it a versatile tool for both basic research and potential therapeutic applications.

## RESULTS

### Generation of cCas12a by covalent conjugation of site-specifically azido-modified Cas12a mutant and 5′-DBCO-modified crRNA

It has been demonstrated that extending or otherwise modifying the 5′ terminus of Cas12a crRNA does not affect its activity (Lee et al., 2017; Swarts et al., 2017; Bin Moon et al., 2018), so we began by attempting to covalently link the 5′ terminus of crRNA to Cas12a (Figure 2A). Inspection of the crystal structure of *Acidaminococcus* sp. Cas12a (AsCas12a) in complex with crRNA and target DNA (PDB: 5B43) suggested that M806, which is approximately 6 Å heading to the phosphate group oxygen of A43, might be a suitable conjugation site and that covalent linkage at this site would not interfere with the protein-RNA interaction (Figure 2B). Noncanonical amino acid mutagenesis was applied to prepare the Cas12a mutant by replacing the methionine residue at 806 position with an azide-containing ncAA, 4-(2-azidoethoxy)-l-phenylalanine (AeF) (Figure 2C), as described previously (Ling et al., 2020b). Briefly, the M806 codon was mutated to TAG, and the mutant protein was expressed in *Escherichia coli* BL21 cells in the presence of an engineered *Methanococcus jannaschii* TyrRS/$tRNA_{CUA}$ pair (Tang et al., 2018). The expression yield of the M806AeF mutant (designated AzCas12a) was 15 mg/L, which is comparable with that of the WT protein. The incorporation of AeF and its precise location were validated using mass spectrometry (Figure 2D). The nuclease activity, stability, and genome cleavage efficiency of the WT and mutant proteins were assessed using *in vitro* DNA cleavage assay (Figures S1A and S1B), differential scanning fluorimetry (Figure S1C), and enhanced green fluorescent protein (EGFP) gene disruption assay in HEK293-EGFP-TetOn cells (Ling et al., 2020c) (Figure S1D). In summary, AzCas12a mutant showed identical activity to that of the WT Cas12a nuclease.

Next, we covalently attached 5′-DBCO-modified crRNA (Figure S1E) to AzCas12a by means of a site-specific strain-promoted alkyne-azide cycloaddition reaction. As shown in Figure 2E, SDS-PAGE analysis revealed a significant band-shift only for the RNP complex containing AzCas12a and 5′-DBCO-modified crRNA, and the reaction was almost quantitative. The nuclease activity of cCas12a RNP was confirmed using a DNA cleavage assay *in vitro* (Figure 2F). Taken together, these results demonstrate that cCas12a RNP could be prepared simply by mixing the two components and the resulting cCas12a RNP retained the activity of the WT Cas12a RNP.

### CRISPR/cCas12a displays increased genome editing efficiency in human and mouse cells

To investigate the genome editing efficiency by covalent strategy in mammalian cells, cCas12a RNP was evaluated in HEK293-EGFP-TetOn cells using an EGFP disruption assay (Figure 3A). First, we evaluated unconjugated RNPs consisting of either WT Cas12a or AzCas12a and found that they showed EGFP gene disruption efficiencies of 21.7% and 22.3%, respectively; in contrast, the RNP consisting of AzCas12a conjugated with 5′-DBCO-modified crRNA showed an efficiency of more than 66.8%, which is approximately a 3-fold increase of activity. Next, we examined the editing activities on five endogenous gene loci in HEK293 cells. Conjugated RNPs showed an editing efficiency increase of 1.6- to 18.3-fold than the WT Cas12a RNP at all five sites (Figure S1F). To further explore the effects of covalent conjugation, we also evaluated the genome editing efficiencies of the cCas12a RNP in three hard-to-transfect cell types—K562, Jurkat, and NIH/3T3—as model systems to explore the possible utility of cCas12a-crRNA conjugates in leukemia disease treatment, T cell engineering, and animal model

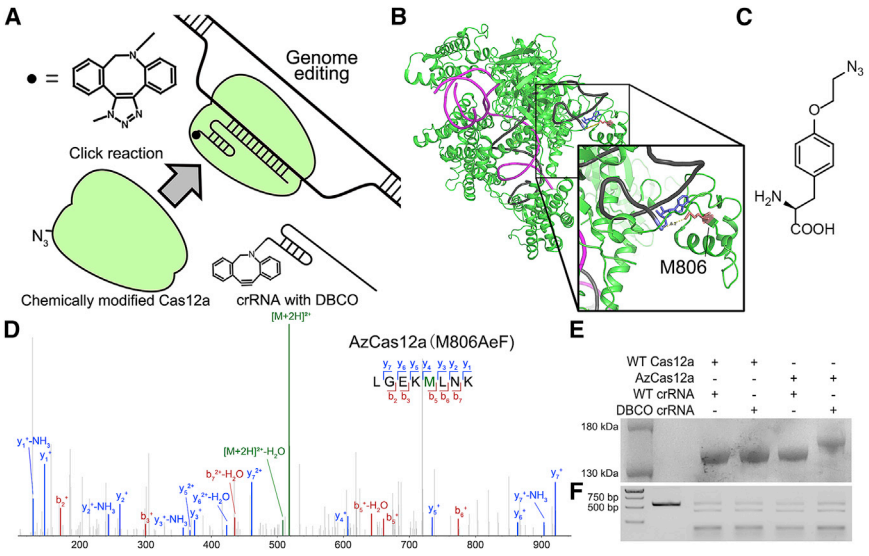



**Figure 2. Generation of site-specific azido-modified Cas12a and covalent linkage with 5′ modified crRNA**

(A) Schematic illustration of the chemical conjugation strategy. Cas12a mutant containing an azide moiety at M806 position, introduced by noncanonical amino acid mutagenesis, was reacted with 5′-DBCO-modified crRNA to form a covalent complex.

(B) Crystal structure of *Acidaminococcus* sp. Cas12a in complex with crRNA and target DNA (PDB: 5B43). The residue selected for AeF mutagenesis (M806) is labeled in red, and the 5′ terminal base is labeled in blue. The distance between AeF and the base backbone was measured using PyMOL.

(C) Chemical structure of noncanonical amino acid AeF.

(D) Tandem mass spectrometry (MS/MS) fragmentation of peptides derived from AzCas12a. The correct MS spectrum confirmed that AeF had been incorporated at the M806 site; the mutation site is labeled with a green M.

(E) SDS-PAGE analysis of the reaction product between AzCas12a and 5′-DBCO-modified crRNA. The reaction was performed at 4°C for 3 h by mixing the protein and RNA at equal stoichiometry.

(F) Nuclease activity of WT Cas12a and AzCas12a RNPs *in vitro*. Double-stranded DNA was digested in the presence of a pre-assembled ribonucleoprotein complexes for 1 h at 37°C.

construction, respectively. Human HPRT1 (hHPRT1) locus in the K562 cell line was first tested as a target, and genome editing efficiencies were analyzed using T7E1 assay (Figure 3B). We found that WT Cas12a in complex with either WT crRNA or 5′-DBCO-modified crRNA showed genome editing efficiencies of 10.6% and 12.9%, respectively, whereas the editing efficiency of the cCas12a RNP was 44.1%, which represents a 4-fold increase. Similarly, in Jurkat cells, the editing efficiency of the WT Cas12a RNP targeting the hHPRT1 locus was 26.3%, whereas that of the cCas12a RNP was 51.5% (Figure 3C), which is an approximately 2-fold improvement. Besides human cells, mouse NIH/3T3 cell were also treated with Cas12a RNP complex containing crRNA targeting the mouse HPRT1 (mHPRT1) gene. As shown in Figure 3D, the editing efficiencies of WT Cas12a and cCas12a RNP complex were 8.0% and 25.4%, respectively. Taken together, these results demonstrate that covalently linking crRNA to Cas12a could indeed substantially increase genome editing efficiency in different cells at different loci.

## Evaluating the off-target effects of CRISPR/cCas12a

An increase of on-target cleavage efficiency will likely increase the risk for off-target effects. To evaluate this possibility, we first applied the most commonly used method, GUIDE-seq (Tsai et al., 2015), to assess the on-target and off-target frequencies of the cCas12a and WT Cas12a RNPs targeting three different gene loci, hHPRT1, GUK1, and DNMT1 genes, in HEK293 cells (Figure 3E). The results confirmed that the on-target reads increased by 2- to 6-fold in three different loci for cCas12a. The AsCas12a system has been demonstrated to be highly specific in human cells, and off-target cleavage is difficult to detect for most of the tested crRNAs (Kleinstiver et al., 2016; Chen et al., 2020). Indeed, no off-target cleavage was detected in cCas12a targeting hHPRT1 and GUK1 loci (Figure 3E). For crRNA targeting DNMT1, which is arbitrarily chosen because of its high off-target cleavage in cells (Kleinstiver et al., 2016; Bin Moon et al., 2018), we indeed detected significant increase in off-target cleavage in cCas12a-treated cells. This particular site is known for its high off-target cleavage due to the poor intrinsic sequence specificity (Kleinstiver et al., 2016). As genome cleavage can mediate chromosomal translocation, which poses great threats to genome integrity, we also applied a recently developed primer extension-mediated sequencing (PEM-seq) method (Yin et al., 2019) on this DNMT1 site. PEM-seq can detect not only off-target DNA cleavage but also chromosomal translocations and large deletions. The results showed that only one off-target DNA cleavage site was detected in both the cCas12a group and WT group and that there is no difference in the average percentages of genome-wide translocations and large deletions between the two groups (Figure 3F; Figure S2). To give more evidence, a biochemical method, SITE-seq (Cameron et al., 2017), was also applied to evaluate the off-target effect using DNMT1 and GUK1 gene loci in HEK293 cells. As shown in Figure 3G, no difference in off-target reads in GUK1 loci was observed, while the on-target reads were increased by 2.6-fold. Again, on the DNMT1 site, more off-target cleavage sites were detected in the cCas12a-treated group. Overall, these data suggested that covalent linkage of the RNP complex indeed can increase the on-target genome editing efficiency, while the risk for off-target effects may depend on the intrinsic sequence specificities of the crRNAs.

## The covalent strategy can be applied to other Cas12a family proteins for improving editing efficiency

To explore whether our covalent strategy could be applied to other Cas12a family proteins for enhancing genome editing efficiency, we chose *Lachnospiraceae bacterium* Cas12a

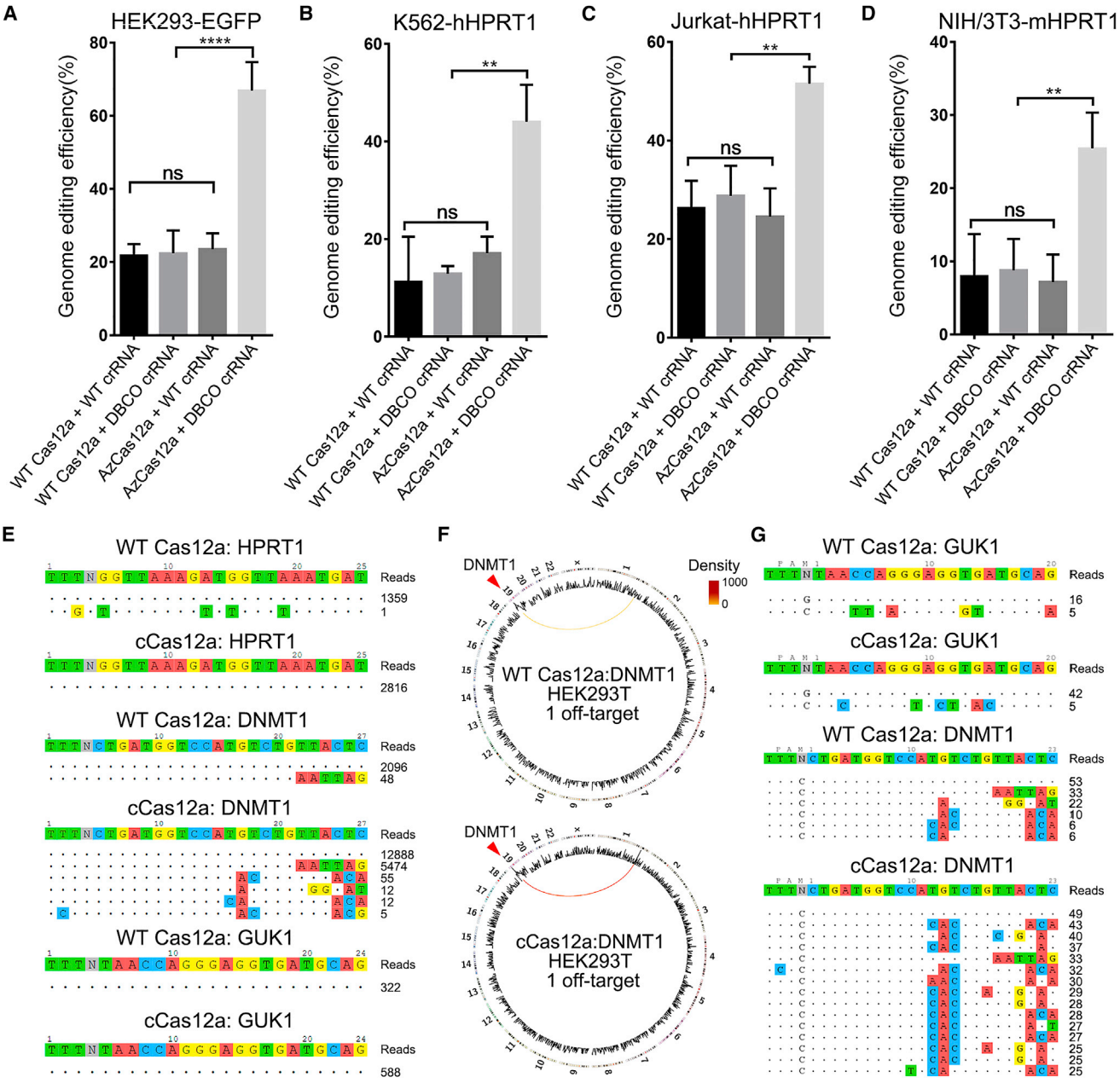



**Figure 3. cCas12a showed increased genome editing efficiency compared with WT Cas12a without increase of off-target effect**

(A) HEK293-EGFP-TetOn cells were treated with different RNPs (WT Cas12a or AzCas12a paired with WT or 5′-DBCO-modified crRNA at 45 pmol) by electroporation. Flow cytometry analysis was performed 48 h after treatment, and genome editing efficiencies were quantified by fluorescence decreases. Data are presented as mean ± SEM derived from triplicate samples (n = 3). Statistical significance is determined using a two-tailed Student's t test: ****$p < 0.0001$.

(B–D) K562 (B), (C) Jurkat, and (D) NIH/3T3 cells were treated with different RNPs (45 pmol). Editing efficiencies were measured using T7E1 assay 48 h after electroporation. Data are from three independent biological replicates. Error bars indicate ±SEM. Statistical significance is determined using a two-tailed Student's t test: **$p < 0.01$.

(E) On-target and off-target efficiencies evaluated using GUIDE-seq with crRNA targeting the hHPRT1, DNMT1, and GUK1 loci.

(F) Circos plots for detection of WT Cas12a and cCas12a off-target effects by primer extension-mediated sequencing with crRNA targeting the DNMT1 locus. Three biological replicates are shown from outside to inside. Red arrows indicate sites where DNMT1 was cleaved by Cas12a. The colored curved lines connect the on-target site to the off-target site.

(G) On-target and off-target efficiencies evaluated using Site-seq with crRNA targeting the human DNMT1 and GUK1 locus.

(LbCas12a) for additional tests. Inspection of the crystal structure of LbCas12a in complex with a crRNA and its target DNA (PDB: 5XUU) revealed H759 to be a potentially appropriate conjugation site (Figure S3A). An H759AeF mutant enzyme was generated and purified for further RNA conjugation and evaluation. To assess the editing efficiency in mammalian cells, WT LbCas12a and conjugated LbCas12a RNPs containing RNA targeting EGFP gene were delivered into HEK293-EGFP-TetOn cells through electroporation. The EGFP quenching percentage of the conjugated LbCas12a RNP (28.3%) was 1.7 times greater than that of the WT RNP (17.0%), indicating that the covalent strategy was indeed effective in this system (Figure S3B). These results confirm that the covalent conjugation strategy could be used in other Cas12a family members.

## The covalent strategy can improve the activities of enhanced Cas12a mutants and Cas12a-based base editors

Next, we explore whether our covalent strategy could be applied to other existing state-of-the-art Cas12a mutants. A recent reported activity and targeting ranges improved version of Cas12a (Kleinstiver et al., 2019) was prepared as an M806AeF mutant (termed as AzenAsCas12a). As shown in Figure S3, the covalent linkage can indeed improve the genome editing efficiency of the enhanced Cas12a mutant. The genome editing efficiency of cCas12a and WT Cas12a were further validated using next-generation sequencing (Figure S3F). Collectively, these data demonstrated that covalent strategy could be compatible with existing methods to improve the Cas12a-based genome editing system.

Base editors have emerged as next-generation genome editing tools, and recently, Cas12a-derived base editors have been developed to induce base editing in mammalian cells (Li et al., 2018; Kleinstiver et al., 2019; Wang et al., 2020). To determine whether our covalent conjugation strategy could also work on Cas12a-based base editor, we recombinantly expressed a site-specific azido-modified AsCas12a base editing protein (Cas12a-BE) (Kleinstiver et al., 2019) (Figure S3G). A crRNA targeting the human FANCF gene was applied to evaluate the level of cytosine-to-thymine conversion. The sequencing results showed that conjugated Cas12a-BE RNP can indeed increases the base editing efficiency compared with the WT system (Figure S3H). To further confirm the effects of covalent conjugation on base editing, we evaluated three additional sites. For all sites tested, the base editing efficiency was increased by 1.5- to 2-fold (Figure S3I). Overall, these results confirmed that the cCas12a system could improve the efficiency of Cas12a-based base editors.

## CRISPR/cCas12a increases HDR-mediated precise gene knockin efficiency

Cas12a cleaves target DNA far away from the PAM and provides additional opportunity to cut at the target site after indel formation, thus enhancing the chance of homology-directed repair (HDR)-mediated gene integration. To explore whether the cCas12a RNP also showed improved HDR efficiency, we co-electroporated the cCas12a RNP and a single-strand donor DNA carrying an EcoRI recognition site targeting the hHPRT1 locus into HEK293 cells (Figure 4A). Successful HDR-mediated knockin of the donor DNA could be detected by means of PCR amplification followed by EcoRI digestion and agarose gel electrophoresis. As shown in Figure 4B, the knockin efficiencies achieved with WT Cas12a and cCas12a RNPs at 40 and 60 pmol were 2.2%, 3.4%, 17.9%, and 22.5%, respectively. The HDR efficiency for the covalently conjugated complex was 7–8 times than that for the unconjugated complex. To provide more evidence, we evaluated the EcoRI fragment knockin on four additional genomic loci. The HDR efficiencies are 0.7%–4.6% and 5.2%–22.5% for WT Cas12a and cCas12a RNPs treatments, respectively (Figure S4A), which are 2.9- to 7.4-fold increases. Collectively, these results confirmed that the conjugation strategy could improve Cas12a-based HDR efficiency in mammalian cells.

## cCas12a increases site-specifically integrated CAR-T cell preparation efficiencies

Genome editing in human primary T cells holds promise for improving current and developing immunotherapeutic strategies (June and Sadelain, 2018). Currently approved CAR-T cell preparations are based on randomly integrated lentiviral and $\gamma$-retroviral vectors and thus carry the risk for insertional mutagenesis-induced carcinogenesis and translational dysregulation (Howe et al., 2008; Wang and Rivière, 2016). Therefore, attempts have recently been made to use gene editing techniques to create more consistent and robust CAR-T cells in precise genome locus (Eyquem et al., 2017; Stadtmauer et al., 2020). Compared with Cas9, Cas12a has been reported to be not only safer and more precise (Strohkendl et al., 2018) but also more efficient when CAR-T cells are prepared by Cas12a mRNA electroporation followed by adeno-associated virus (AAV)-mediated donor DNA delivery (High and Anguela, 2016; Dai et al., 2019; Moço et al., 2020). To determine whether our cCas12a platform could be used to facilitate CAR-T cell preparation, we carried out experiments involving Cas12a RNP electroporation followed by AAV-mediated donor DNA delivery. Specifically, we designed a Cas12a RNP targeting the endogenous T cell receptor (TCR) so that an approximately 2.5 kb DNA cassette could be integrated into the 5′ end of the first exon of the TCR-$\alpha$ constant region. The donor DNA containing an anti-CD19 CAR with a Myc tag was delivered using AAV6 (Figure 4C). For a proof-of-concept study, RNPs at various concentrations were electroporated into Jurkat cells, which were then infected with AAV (multiplicity of infection = $10^6$), and the CAR knockin efficiency was measured using anti-Myc antibody immunofluorescent staining. As shown in Figure S4B, Jurkat cells treated with an increasing amount of cCas12a showed CAR-positive ratios of 56.8% and 81.1%, whereas the WT groups showed CAR-positive ratios of 28.0% and 55.5% under the same conditions. To confirm that the CAR sequence was indeed knocked into the Jurkat cell genome at the desired location, we used previous reported semiquantitative in-and-out PCR method to determine the integration efficiency (Dai et al., 2019). At the tested concentrations, the conjugated Cas12a showed markedly higher CAR knockin efficiency at the genomic DNA level compared with the WT enzyme (Figure S4C), which is consistent with the immunofluorescent staining results. Next, we

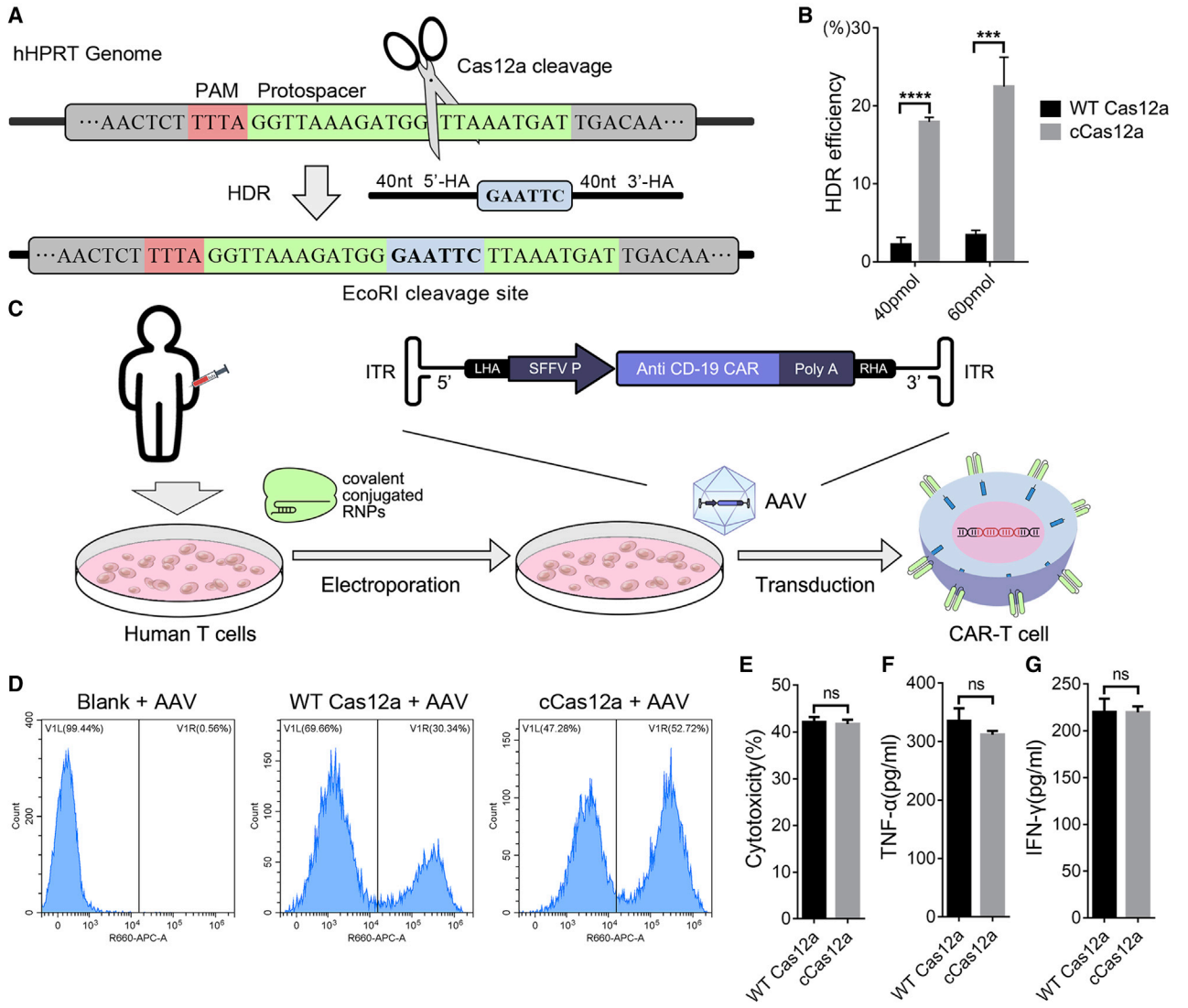



**Figure 4. High-efficiency generation of site-specific genome knockin and CAR-T preparation with cCas12a**

(A) Evaluation of HDR efficiency by knockin of an EcoRI recognition site at the human HPRT1 locus.

(B) HDR efficiencies of WT Cas12a and cCas12a RNPs (40 and 60 pmol). The RNPs and a single-stranded oligo donor (24 and 36 pmol) were co-electroporated into HEK293 cells, and HDR efficiency was measured by means of target amplification and EcoRI digestion. Data are presented as mean ± SEM derived from triplicate samples (n = 3). Statistical significance is determined using a two-tailed Student's t test: ***$p < 0.001$ and ****$p < 0.0001$.

(C) Schematic representation of cCas12a electroporation combined with AAV-delivered HDR template enabling anti-CD19 CAR knockin in human primary T cells.

(D) Flow cytometry analysis of CAR knockin efficiency. T cells were stained with anti-Myc antibody and analyzed using flow cytometry.

(E) *In vitro* cytotoxic activity of CAR-T cells on NALM6 cancer cells was measured using LDH-Glo Cytotoxicity assay, with an effector/target ratio of 10:1. Data are presented as mean ± SEM derived from triplicate samples (n = 3). Statistical significance is determined using a two-tailed Student's t test. ns, not significant.

(F) Cytokine expression levels in CAR-T cells prepared with WT Cas12a or cCas12a RNP. Anti-CD19 CAR-T cells and NALM6 cells were co-cultured for 24 h before evaluation, and levels of interferon-$\gamma$ and tumor necrosis factor-$\alpha$ were measured using ELISA. Data are presented as mean ± SEM derived from triplicate samples (n = 3). Statistical significance is determined using a two-tailed Student's t test. ns, not significant.

used the same procedure to engineer freshly prepared human primary T cells (Figure 4C). WT Cas12a and cCas12a RNPs were electroporated into T cells, which were then infected with AAV 3 days after initial activation. Five days after electroporation, the CAR knockin efficiency was measured using flow cytometry (Figure 4D). This analysis revealed that WT Cas12a treatment generated anti-CD19 CAR-T cells with efficiency of 30.3%, and the efficiency for cCas12a was 52.7%. These results were confirmed on the genome level with semiquantitative in-and-out PCR (Figure S4D). To evaluate the immunological characteristics, we sorted the CAR-positive cells made by WT Cas12a and cCas12a to normalize the CAR-positive T cell ratio and assess the cytolytic activity and the cytokine production activities using a cognate cancer cell line, NALM6 (CD19+). The immunological characteristics of CAR-T prepared by cCas12a were identical to that of WT Cas12a (Figures 4E and 4F). The above-described

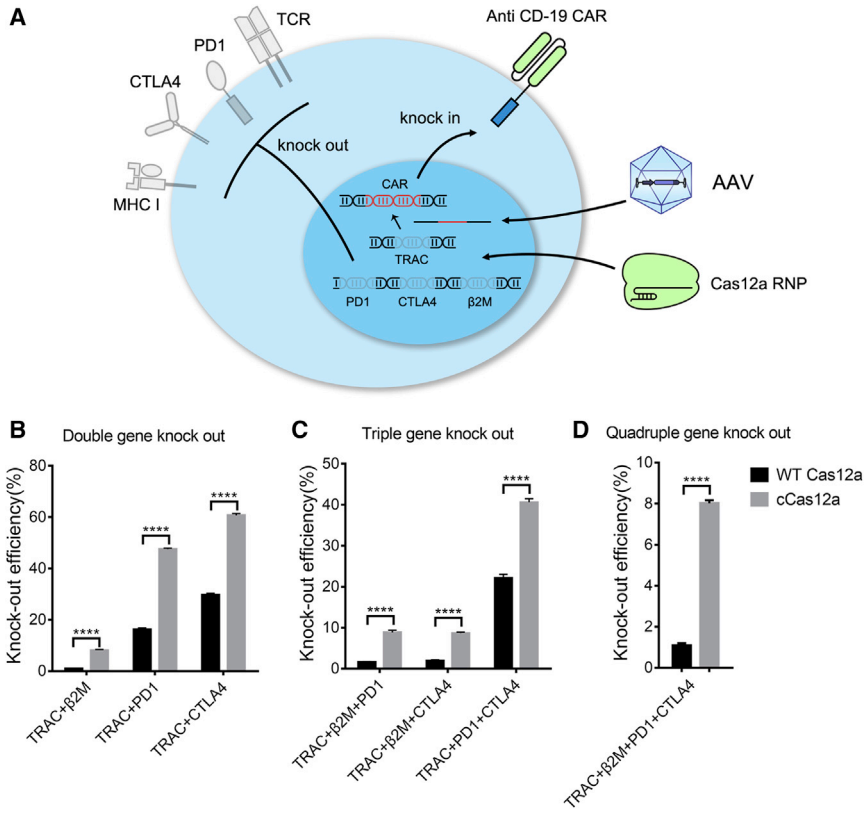



**Figure 5. High-efficiency generation of universal CAR-T with cCas12a-mediated multiplexed gene editing**

(A) Schematic representation of universal CAR-T cells resistant to PD1 and CTLA4 preparation. Thirty picomolar WT Cas12a or cCas12a against TRAC (endogenous TCR disruption), β2M (endogenous MHC-I disruption), PD1 (PD1 disruption), and CTLA4 (CTLA4 disruption) were prepared individually and mixed before electroporation into primary T cells. 4 h after electroporation, T cells were transduced with AAV (MOI = $1 \times 10^6$) to deliver HDR template for anti-CD19 CAR knockin.

(B–D) Quantitative analysis of multiplex genome disruption efficiency. (B) Double-gene knockout, (C) triple-gene knockout, and (D) quadruple-gene knockout T cells were stained with APC anti-human CD3, FITC anti-human β2-microglobulin, PE anti-human CD279, and PE/Cyanine 7 anti-human CD152, and data were analyzed using flow cytometry 5 days after electroporation. Data are presented as mean ± SEM derived from triplicate samples (n = 3). Statistical significance is determined using a two-tailed Student's t test: ****$p < 0.0001$.

experiments demonstrate that the cCas12a system improved the efficiency of CAR-T cell preparation, and T cells treated with cCas12a presented the same immunological characteristics as that of the WT Cas12a system, suggesting that this system has potential utility for T cell engineering.

## High-efficiency multiplex genome editing to generate universal CAR-T cells by cCas12a

The majority of current CAR-T clinical trials use autologous T cells, which are hampered by the poor quality and quantity of patent T cells, as well as the time and expense of manufacturing the autologous T cell products. These limitations would be circumvented by using allogeneic T cells as a universal CAR-T treatment (Depil et al., 2020). CRISPR-based systems have recently emerged as a simple and efficient way for multiplex genome engineering in universal CAR-T preparation (Liu et al., 2017; Ren et al., 2017a, 2017b; Dai et al., 2019; Stadtmauer et al., 2020). To determine whether the cCas12a platform could be used to facilitate universal CAR-T cell preparation, we designed Cas12a RNP targeting endogenous TRAC, β-2 microglobulin (β2M), PD1, and CTLA4 simultaneously, to generate gene-disrupted allogeneic CAR-T cells deficient in TCR, MHC class I molecule, and T cell exhausting molecules (Figure 5A). Multiplex gene knockout was first tested in Jurkat cells. WT Cas12a and cCas12a were electroporated into Jurkat cells, and the editing efficiency was analyzed using T7E1 assay. As shown in Figure S5A, cCas12a group showed higher efficiency for multiplex gene editing compared with WT Cas12a group. In detail, cCas12a showed 2-fold gene knockout efficiency compared with WT Cas12a for simultaneous double knockout (TRAC paired with β2M, PD1, or CTLA4). For simultaneous triple-gene knockout, WT Cas12a and cCas12a treatment showed editing efficiency of 3.3% and 17.3% for TRAC, β2M, and PD1 triple knockout; 2.1% and 25.1% for TRAC, β2M, and CTLA4 triple knockout; and 11.2% and 39.5% for TRAC, PD1, and CTLA4 triple knockout. Overall, cCas12a showed a 3.5- to 12-fold increase of genome editing efficiency for simultaneous triple-gene knockout compared with WT Cas12a. For simultaneous quadruple-gene knockout, covalent conjugation increases the editing efficiency by 8.7-fold. Next, we evaluated cCas12a-mediated multiplex genome editing on primary T cells. WT Cas12a or cCas12a RNP targeting different gene loci were electroporated into T cells followed by AAV transduction to generated universal CAR-T cells. Five days after electroporation, multiplex gene knockout efficiency and anti-CD19 CAR knockin efficiency were quantified using flow cytometry. As shown in Figure 5B, for simultaneous two-gene knockout, cCas12a showed average 2.0- to 8.6-fold editing efficiency improvement compared with WT Cas12a: 8.6-fold for TRAC and β2M, 2.9-fold for TRAC and PD1, and 2.0-fold for TRAC and CTLA4 double knockout (Figure S5B). For simultaneous three-gene knockout, cCas12a increases the editing efficiency by 5.4-fold for TRAC, β2M, and PD1; 4.4-fold for TRAC, β2M, and CTLA4; and 1.8-fold for TRAC, PD1, and CTLA4 triple knockout compared with the WT complex (Figure S5C). Finally, for universal CAR-T preparation with simultaneous four-gene knockout, cCas12a showed an overall 7.4-fold editing efficiency improvement compared with WT Cas12a (Figure S5D). These data demonstrated that multiplex genome

editing to generate universal CAR-T cells could be achieved with cCas12a at high efficiency. Meanwhile, CD19 CAR knockin efficiency was determined to be 28.0% and 36.8% in the WT Cas12a and cCas12a groups, respectively, resulting in a final 9.7-fold increase of quadruple-gene knockout and CAR knockin T cells (Figure S5E).

## DISCUSSION

Although Cas12a has shown potential to be a superior alternative to Cas9 because of the higher precision in genome editing and the ability to recognize different protospacer adjacent motif sequences, its performance for single-site editing is unsatisfactory, which has hampered its broad application. In this work, we demonstrated that Cas12a and crRNA can be covalently linked into one piece, which effectively turns a three-component DNA cleavage reaction into a two-component one. Precise control over the conjugation site and geometry could be achieved by noncanonical amino acid mutagenesis to introduce an azide reaction handle into a designed location on Cas12a, and the azido group was subsequently linked with 5′-DBCO-modified crRNA through biorthogonal reaction. This process generated a conjugated RNP that retained the *in vitro* activity of the WT RNP. Once delivered into cells, the cCas12a showed genome editing efficiency several times greater than that of the WT Cas12a. The higher editing efficiency of cCas12a was observed in several different types of cells and at various target loci. In addition, we observed much higher HDR efficiency (7- to 8-fold) with cCas12a than that for the WT Cas12a, which prompted us to use this method for site-specific CAR-T cell preparation. By combining cCas12a with an AAV donor delivery system, we achieved precise CAR knockin and a T cell preparation efficiency exceeding 50%. Furthermore, the cCas12a successfully improved the allogeneic universal CAR-T preparation efficiency with multiplex gene editing 10-fold compared with the WT complex. This system provides a useful tool for efficient mammalian cell engineering and may have potential clinical applications not only for T cells but also for other clinically relevant cell types.

### Limitations of the study

The covalent conjugation strategy may have several limitations. First, as the chemically modified proteins are recombinantly expressed and the modified crRNAs are chemically synthesized, its use may be limited in certain applications that require genetic expression of the CRISPR components. However, for many applications, RNP delivery is a prevalent and preferred method that exhibits several advantages (high efficiency and safety) compared with genetically encoded CRISPR system (Zuris et al., 2015; Chen et al., 2016; Rouet et al., 2018).

Second, at least for one crRNA sequence, DNMT1, a site that is known for off-target detection using Cas12a system, we detected an increase of off-target cleavage along with increased on-target cleavage efficiency. This is likely to be a result of the intrinsic sequence property or specificity of the crRNA. As most crRNAs for Cas12a have no detectable off-target cleavage (Kleinstiver et al., 2019), with the development of better crRNA design algorithms and tools, such crRNAs with high off-target risk could be avoided.

Finally, it is unclear whether such covalent strategy could also benefit other CRISPR family members. In the case of Cas9, because of the high editing efficiency and picomolar binding affinity between Cas9 and the long single guide RNA, we would not expect the effect of covalent conjugation to be significant. With the discovery of more Cas family proteins with smaller size and shorter crRNA, such as the recently discovered Casφ protein (Pausch et al., 2020), the covalent strategy may possibly be applied to stabilize the complex and increase its genome editing efficiency. More structural information and biochemical characterization of these Cas family members should facilitate the rational design of the conjugation site and promote this method to be generally applied. We also hope that this covalent linkage idea, which has never been explored before, will inspire more creative designs, such as ones that can be used in genetically encoded CRISPR systems, to improve other genome editing systems in the future.

## STAR★METHODS

Detailed methods are provided in the online version of this paper and include the following:

- KEY RESOURCES TABLE
- RESOURCE AVAILABILITY
  - Lead contact
  - Materials availability
  - Data and code availability
- EXPERIMENTAL MODEL AND SUBJECT DETAILS
  - Cell culture
- METHOD DETAILS
  - General information
  - Plasmid construction
  - Protein expression and purification
  - *In vitro* transcription of crRNA
  - Protein melting point analysis
  - *In vitro* DNA cleavage assay
  - *In vitro* RNP assembled and electroporated in cell lines
  - EGFP disruption assay and flow cytometry analysis
  - Genomic DNA purification and PCR amplification
  - T7E1 cleavage assay
  - Off-target detection by Guide-seq
  - Off-target detection by Site-seq
  - Off-target detection by PEM-seq
  - HDR complex preparation and electroporation
  - Cas12-BE RNP preparation and cell electroporation
  - AAV production and purification
  - CAR-Jurakt / CAR-T cell preparation
  - LDH-Glo cytotoxicity assay
  - Immunological characteristic of CAR-T cells
  - Semiquantitative in-and-out PCR
  - NGS sequencing
  - Multiplex gene editing in Jurkat and T cell
- QUANTIFICATION AND STATISTICAL ANALYSIS
  - T7E1 cleavage assay quantification
  - EcoRI knock-in efficiency evaluation
  - Flow cytometry analysis of CAR knock in efficiency
  - LDH-Glo cytotoxicity quantification

- Cell viability quantification
- Flow cytometry analysis of T cell for multiple gene editing
- Statistical analysis

- ADDITIONAL RESOURCES
  - Detailed protocol

## SUPPLEMENTAL INFORMATION

Supplemental information can be found online at https://doi.org/10.1016/j.molcel.2021.09.021.

## ACKNOWLEDGMENTS

This work was financially supported by National Natural Science Foundation of China (91853111, 21922701, 21778005, and 31771485), the Beijing Natural Science Foundation (JQ20034), the National Major Scientific and Technological Special Project for "Significant New Drugs Development" (2019ZX09739001), the Shenzhen Institute of Synthetic Biology Scientific Research Program (DWKF20190004), and the Peking University and Innovation Fund for Outstanding Doctoral Candidates of Peking University Health Science Center (71006Y2460). We acknowledge Dr. Xiaomeng Shi and Xiaohui Zhang at the State Key Laboratory of Natural and Biomimetic Drugs for assistance with high-resolution protein mass spectrometry and Prof. Quan Du from the Peking University School of Pharmaceutical Sciences for kindly providing the pCDNA3.1 AsCas12a plasmid.

## AUTHOR CONTRIBUTIONS

X.L. and T.L. designed the experiments. X.L., L.C., H.C., X.G., and Y.Z. performed plasmid construction, protein expression and purification, mass spectrometry, and activity assays. H.C. performed chemical synthesis and base editing evaluation. X.L., L.C., and H.C. performed electroporation and mammalian cell genome editing. X.L., L.C., and B.Z. performed CAR-T cell preparation and evaluation. X.L., J.Y., and J.H. performed the off-target assays and analyzed the data. X.L. and T.L. wrote the paper.

## DECLARATION OF INTERESTS

The authors declare no competing interests.

Received: February 1, 2021
Revised: June 28, 2021
Accepted: September 16, 2021
Published: October 13, 2021

## REFERENCES

Agard, N.J., Prescher, J.A., and Bertozzi, C.R. (2004). A strain-promoted [3 + 2] azide-alkyne cycloaddition for covalent modification of biomolecules in living systems. J. Am. Chem. Soc. *126*, 15046–15047.

Anzalone, A.V., Koblan, L.W., and Liu, D.R. (2020). Genome editing with CRISPR-Cas nucleases, base editors, transposases and prime. Nat. Biotechnol. *38*, 824–844.

Bin Moon, S., Lee, J.M., Kang, J.G., Lee, N.-E., Ha, D.-I., Kim, D.Y., Kim, S.H., Yoo, K., Kim, D., Ko, J.-H., and Kim, Y.S. (2018). Highly efficient genome editing by CRISPR-Cpf1 using CRISPR RNA with a uridinylate-rich 3′-overhang. Nat. Commun. *9*, 3651.

Cameron, P., Fuller, C.K., Donohoue, P.D., Jones, B.N., Thompson, M.S., Carter, M.M., Gradia, S., Vidal, B., Garner, E., Slorach, E.M., et al. (2017). Mapping the genomic landscape of CRISPR-Cas9 cleavage. Nat. Methods *14*, 600–606.

Chen, S., Lee, B., Lee, A.Y.-F., Modzelewski, A.J., and He, L. (2016). Highly efficient mouse genome editing by CRISPR ribonucleoprotein electroporation of zygotes. J. Biol. Chem. *291*, 14457–14467.

Chen, J.S., Ma, E., Harrington, L.B., Da Costa, M., Tian, X., Palefsky, J.M., and Doudna, J.A. (2018). CRISPR-Cas12a target binding unleashes indiscriminate single-stranded DNase activity. Science360, 436–439.

Chen, P., Zhou, J., Wan, Y., Liu, H., Li, Y., Liu, Z., Wang, H., Lei, J., Zhao, K., Zhang, Y., et al. (2020). A Cas12a ortholog with stringent PAM recognition followed by low off-target editing rates for genome editing. Genome Biol. *21*, 78.

Chin, J.W. (2017). Expanding and reprogramming the genetic code. Nature *550*, 53–60.

Dai, X., Park, J.J., Du, Y., Kim, H.R., Wang, G., Errami, Y., and Chen, S. (2019). One-step generation of modular CAR-T cells with AAV-Cpf1. Nat. Methods *16*, 247–254.

Depil, S., Duchateau, P., Grupp, S.A., Mufti, G., and Poirot, L. (2020). 'Off-the-shelf' allogeneic CAR T cells: development and challenges. Nat. Rev. Drug Discov. *19*, 185–199.

Dominguez, A.A., Lim, W.A., and Qi, L.S. (2016). Beyond editing: repurposing CRISPR-Cas9 for precision genome regulation and interrogation. Nat. Rev. Mol. Cell Biol. *17*, 5–15.

Dong, D., Ren, K., Qiu, X., Zheng, J., Guo, M., Guan, X., Liu, H., Li, N., Zhang, B., Yang, D., et al. (2016). The crystal structure of Cpf1 in complex with CRISPR RNA. Nature *532*, 522–526.

Dumas, A., Lercher, L., Spicer, C.D., and Davis, B.G. (2015). Designing logical codon reassignment - Expanding the chemistry in biology. Chem. Sci. (Camb.) *6*, 50–69.

Eyquem, J., Mansilla-Soto, J., Giavridis, T., van der Stegen, S.J.C., Hamieh, M., Cunanan, K.M., Odak, A., Gönen, M., and Sadelain, M. (2017). Targeting a CAR to the TRAC locus with CRISPR/Cas9 enhances tumour rejection. Nature *543*, 113–117.

High, K.A., and Anguela, X.M. (2016). Adeno-associated viral vectors for the treatment of hemophilia. Hum. Mol. Genet. *25* (R1), R36–R41.

Howe, S.J., Mansour, M.R., Schwarzwaelder, K., Bartholomae, C., Hubank, M., Kempski, H., Brugman, M.H., Pike-Overzet, K., Chatters, S.J., de Ridder, D., et al. (2008). Insertional mutagenesis combined with acquired somatic mutations causes leukemogenesis following gene therapy of SCID-X1 patients. J. Clin. Invest. *118*, 3143–3150.

Hsu, P.D., Lander, E.S., and Zhang, F. (2014). Development and applications of CRISPR-Cas9 for genome engineering. Cell *157*, 1262–1278.

Jones, S.K., Jr., Hawkins, J.A., Johnson, N.V., Jung, C., Hu, K., Rybarski, J.R., Chen, J.S., Doudna, J.A., Press, W.H., and Finkelstein, I.J. (2021). Massively parallel kinetic profiling of natural and engineered CRISPR nucleases. Nat. Biotechnol. *39*, 84–93.

June, C.H., and Sadelain, M. (2018). Chimeric antigen receptor therapy. N. Engl. J. Med. *379*, 64–73.

Kim, D., Bae, S., Park, J., Kim, E., Kim, S., Yu, H.R., Hwang, J., Kim, J.-I., and Kim, J.-S. (2015). Digenome-seq: genome-wide profiling of CRISPR-Cas9 off-target effects in human cells. Nat. Methods *12*, 237–243, 1, 243.

Kleinstiver, B.P., Tsai, S.Q., Prew, M.S., Nguyen, N.T., Welch, M.M., Lopez, J.M., McCaw, Z.R., Aryee, M.J., and Joung, J.K. (2016). Genome-wide specificities of CRISPR-Cas Cpf1 nucleases in human cells. Nat. Biotechnol. *34*, 869–874.

Kleinstiver, B.P., Sousa, A.A., Walton, R.T., Tak, Y.E., Hsu, J.Y., Clement, K., Welch, M.M., Horng, J.E., Malagon-Lopez, J., Scarfò, I., et al. (2019). Engineered CRISPR-Cas12a variants with increased activities and improved targeting ranges for gene, epigenetic and base editing. Nat. Biotechnol. *37*, 276–282.

Kocak, D.D., Josephs, E.A., Bhandarkar, V., Adkar, S.S., Kwon, J.B., and Gersbach, C.A. (2019). Increasing the specificity of CRISPR systems with engineered RNA secondary structures. Nat. Biotechnol. *37*, 657–666.

Lee, K., Mackley, V.A., Rao, A., Chong, A.T., Dewitt, M.A., Corn, J.E., and Murthy, N. (2017). Synthetically modified guide RNA and donor DNA are a versatile platform for CRISPR-Cas9 engineering. eLife *6*, e25312.

Li, B., Zhao, W., Luo, X., Zhang, X., Li, C., Zeng, C., and Dong, Y. (2017). Engineering CRISPR-Cpf1 crRNAs and mRNAs to maximize genome editing efficiency. Nat. Biomed. Eng. *1*, 0066.

Li, X., Wang, Y., Liu, Y., Yang, B., Wang, X., Wei, J., Lu, Z., Zhang, Y., Wu, J., Huang, X., et al. (2018). Base editing with a Cpf1-cytidine deaminase fusion. Nat. Biotechnol. *36*, 324–327.

Ling, X., Chen, H., Zheng, W., Chang, L., Wang, Y., and Liu, T. (2020a). Site-specific protein modification by genetic encoded disulfide compatible thiols. Chin. Chem. Lett. *31*, 163–166.

Ling, X., Xie, B., Gao, X., Chang, L., Zheng, W., Chen, H., Huang, Y., Tan, L., Li, M., and Liu, T. (2020b). Improving the efficiency of precise genome editing with site-specific Cas9-oligonucleotide conjugates. Sci. Adv. *6*, eaaz0051.

Ling, X., Gao, X., Chang, L., Chen, H., Shi, X., and Liu, T. (2020c). Rational design of minimum CRISPR guide RNA by site-specific Cas9-RNA conjugation. Chem. Commun. (Camb.) *56*, 7515–7518.

Liu, C.C., and Schultz, P.G. (2010). Adding new chemistries to the genetic code. Annu. Rev. Biochem. *79*, 413–444.

Liu, X., Zhang, Y., Cheng, C., Cheng, A.W., Zhang, X., Li, N., Xia, C., Wei, X., Liu, X., and Wang, H. (2017). CRISPR-Cas9-mediated multiplex gene editing in CAR-T cells. Cell Res. *27*, 154–157.

Liu, P., Luk, K., Shin, M., Idrizi, F., Kwok, S., Roscoe, B., Mintzer, E., Suresh, S., Morrison, K., Frazão, J.B., et al. (2019). Enhanced Cas12a editing in mammalian cells and zebrafish. Nucleic Acids Res. *47*, 4169–4180.

Moço, P.D., Aharony, N., and Kamen, A. (2020). Adeno-associated viral vectors for homology-directed generation of CAR-T cells. Biotechnol. J. *15*, e1900286.

Nakade, S., Yamamoto, T., and Sakuma, T. (2017). Cas9, Cpf1 and C2c1/2/3—what's next? Bioengineered *8*, 265–273.

Pausch, P., Al-Shayeb, B., Bisom-Rapp, E., Tsuchida, C.A., Li, Z., Cress, B.F., Knott, G.J., Jacobsen, S.E., Banfield, J.F., and Doudna, J.A. (2020). CRISPR-CasΦ from huge phages is a hypercompact genome. Science *369*, 333–337.

Ren, J., Zhang, X., Liu, X., Fang, C., Jiang, S., June, C.H., and Zhao, Y. (2017a). A versatile system for rapid multiplex genome-edited CAR T cell generation. Oncotarget *8*, 17002–17011.

Ren, J., Liu, X., Fang, C., Jiang, S., June, C.H., and Zhao, Y. (2017b). Multiplex genome editing to generate universal CAR T cells resistant to PD1 inhibition. Clin. Cancer Res. *23*, 2255–2266.

Rostovtsev, V.V., Green, L.G., Fokin, V.V., and Sharpless, K.B. (2002). A stepwise huisgen cycloaddition process: copper(I)-catalyzed regioselective "ligation" of azides and terminal alkynes. Angew. Chem. Int. Ed. Engl. *41*, 2596–2599.

Rouet, R., Thuma, B.A., Roy, M.D., Lintner, N.G., Rubitski, D.M., Finley, J.E., Wisniewska, H.M., Mendonsa, R., Hirsh, A., de Oñate, L., et al. (2018). Receptor-mediated delivery of CRISPR-Cas9 endonuclease for cell-type-specific gene editing. J. Am. Chem. Soc. *140*, 6596–6603.

Stadtmauer, E.A., Fraietta, J.A., Davis, M.M., Cohen, A.D., Weber, K.L., Lancaster, E., Mangan, P.A., Kulikovskaya, I., Gupta, M., Chen, F., et al. (2020). CRISPR-engineered T cells in patients with refractory cancer. Science *367*, eaba7365.

Strohkendl, I., Saifuddin, F.A., Rybarski, J.R., Finkelstein, I.J., and Russell, R. (2018). Kinetic Basis for DNA Target Specificity of CRISPR-Cas12a. Mol. Cell *71*, 816–824.e3.

Swarts, D.C., van der Oost, J., and Jinek, M. (2017). Structural basis for guide RNA processing and seed-dependent DNA targeting and cleavage by CRISPR-Cas12a. Mol. Cell *66*, 221–233.e4.

Tang, H., Dai, Z., Qin, X., Cai, W., Hu, L., Huang, Y., Cao, W., Yang, F., Wang, C., and Liu, T. (2018). Proteomic identification of protein tyrosine phosphatase and substrate interactions in living mammalian cells by genetic encoding of irreversible enzyme inhibitors. J. Am. Chem. Soc. *140*, 13253–13259.

Tsai, S.Q., Zheng, Z., Nguyen, N.T., Liebers, M., Topkar, V.V., Thapar, V., Wyvekens, N., Khayter, C., Iafrate, A.J., Le, L.P., et al. (2015). GUIDE-seq enables genome-wide profiling of off-target cleavage by CRISPR-Cas nucleases. Nat. Biotechnol. *33*, 187–197.

Wang, X., and Rivière, I. (2016). Clinical manufacturing of CAR T cells: foundation of a promising therapy. Mol. Ther. Oncolytics *3*, 16015.

Wang, H., La Russa, M., and Qi, L.S. (2016). CRISPR/Cas9 in genome editing and beyond. Annu. Rev. Biochem. *85*, 227–264.

Wang, X., Ding, C., Yu, W., Wang, Y., He, S., Yang, B., Xiong, Y.-C., Wei, J., Li, J., Liang, J., et al. (2020). Cas12a base editors induce efficient and specific editing with low DNA damage response. Cell Rep. *31*, 107723.

Wright, A.V., Sternberg, S.H., Taylor, D.W., Staahl, B.T., Bardales, J.A., Kornfeld, J.E., and Doudna, J.A. (2015). Rational design of a split-Cas9 enzyme complex. Proc. Natl. Acad. Sci. U S A *112*, 2984–2989.

Wright, A.V., Nuñez, J.K., and Doudna, J.A. (2016). Biology and applications of CRISPR systems: harnessing nature's toolbox for genome engineering. Cell *164*, 29–44.

Yin, J., Liu, M., Liu, Y., Wu, J., Gan, T., Zhang, W., Li, Y., Zhou, Y., and Hu, J. (2019). Optimizing genome editing strategy by primer-extension-mediated sequencing. Cell Discov. *5*, 18.

Zetsche, B., Gootenberg, J.S., Abudayyeh, O.O., Slaymaker, I.M., Makarova, K.S., Essletzbichler, P., Volz, S.E., Joung, J., van der Oost, J., Regev, A., et al. (2015). Cpf1 is a single RNA-guided endonuclease of a class 2 CRISPR-Cas system. Cell *163*, 759–771.

Zuris, J.A., Thompson, D.B., Shu, Y., Guilinger, J.P., Bessen, J.L., Hu, J.H., Maeder, M.L., Joung, J.K., Chen, Z.-Y., and Liu, D.R. (2015). Cationic lipid-mediated delivery of proteins enables efficient protein-based genome editing in vitro and in vivo. Nat. Biotechnol. *33*, 73–80.

## STAR★METHODS

### KEY RESOURCES TABLE

| REAGENT or RESOURCE | SOURCE | IDENTIFIER |
|---|---|---|
| **Antibodies** | | |
| c-Myc Monoclonal Antibody (9E10) | Invitrogen | Cat# MA1-980; RRID: AB_558470 |
| Anti-mouse IgG (H+L), F(ab')2 Fragment (Alexa Fluor® 647 Conjugate) | Cell Signaling Technology | Cat# 4410 |
| APC anti-human CD3 antibody | Biolegend | Cat# 300412; RRID: AB_314066 |
| FITC anti-human beta2-microglobulin antibody | Biolegend | Cat# 316304; RRID: AB_492837 |
| PE anti-human CD279 (PD-1) antibody | Biolegend | Cat# 329906; RRID: AB_940483 |
| PE/Cyanine7 anti-human CD152 (CTLA-4) antibody | Biolegend | Cat# 369613; RRID: AB_2632875 |
| **Bacterial strains** | | |
| NEB® 5-alpha Competent *E. coli* (High Efficiency) | NEB | Cat# C2987I |
| BL21(DE3) Competent *E. coli* | NEB | Cat# C2527H |
| **Biological samples** | | |
| Human PBMC, health donor | N/A | N/A |
| **Chemicals, peptides, and recombinant proteins** | | |
| Gibson Assembly® Master Mix | NEB | Cat# E2611 |
| DpnI | NEB | Cat# R0176 |
| KOD-One PCR Master Mix | TOYOBO | Cat# KMM-101 |
| 2 × Phanta Max Master Mix | Vazyme | Cat# P525-01 |
| IPTG | Inalco Pharmaceuticals | Cat# 1758-1400 |
| Ni-NTA Agarose | QIAGEN | Cat# 30230 |
| Electroporation buffer | Celetrix LLC, Manassas VA | Cat# 13-0104 |
| 0.4% Trypan Blue Solution | GIBCO | Cat# 15250061 |
| Dulbecco's Modified Eagle's Medium | MACGENE | Cat# CM10013 |
| Fetal Bovine Serum | PAN-Biotech | Cat# P30-3302 |
| RPMI-1640 | MACGENE | Cat# CM10040 |
| Ficoll-Paque PLUS | GE Healthcare | Cat# 17-1440-02 |
| XYbeads Human CD3/CD28 T Cell Activator | SAILY BIO | Cat# XY-B002-001 |
| X-VIVO$^{TM}$15 | Lonza | Cat# 04-418Q |
| Fetal Bovine Serum | GIBCO | Cat# 10099 |
| Human Interleukin-2 | SinoBiological | Cat# GMP-11848-HNAE |
| IL-7 Protein, Human, Recombinant | SinoBiological | Cat# 11821-HNAE |
| IL-15 Protein, Human, Recombinant | SinoBiological | Cat# 10360-HNCE |
| T7 Endonuclease I | Vazyme | Cat# EN303-01 |
| Dimethyl Sulfoxide | SIGMA | Cat# D2650 |
| EcoRI-HF® | NEB | Cat# R3101S |
| CutSmart® buffer | NEB | Cat# B7204S |
| AAV-CD19 CAR | Vigene Biosciences | N/A |
| **Critical commercial assays** | | |
| Dynabeads Untouched Human T Cells Kit | Invitrogen | Cat# 11344D |
| HiScribe T7 High Yield RNA Synthesis Kit | NEB | Cat# E2040S |
| Human IFN gamma Uncoated ELISA kit | Invitrogen | Cat# 88-7316-88 |

(*Continued on next page*)

| *Continued* | | |
|---|---|---|
| REAGENT or RESOURCE | SOURCE | IDENTIFIER |
| Human TNF alpha Uncoated ELISA kit | Invitrogen | Cat# 88-7346-88 |
| LDH-Glo Cytotoxicity Assay | Promega | Cat# J2380 |
| **Deposited data** | | |
| SDS-PAGE in Figure 2E | Mendeley | https://doi.org/10.17632/y5bc6ytjyb.1 |
| Gel in Figure 2F | Mendeley | https://doi.org/10.17632/shsd5hr2d5.1 |
| **Experimental models: Cell lines** | | |
| HEK293 | ATCC | CRL-1573 |
| NIH/3T3 | ATCC | CRL-1658 |
| Jurkat, Clone E6-1 | ATCC | TIB-152 |
| K562 | ATCC | CCL-243 |
| NALM-6 | ATCC | CRL-3273 |
| **Oligonucleotides and gene fragments** | | |
| Primers for PCR and anneal | Genewiz | N/A |
| Synthesized RNA | GENERAL BIOL | N/A |
| ssODN | GENERAL BIOL | N/A |
| CD19-CAR fragment | GENERAL BIOL | N/A |
| **Recombinant DNA** | | |
| pcDNA3.1 AsCas12a | Gifted by Prof. Du Quan | N/A |
| pUltra-MjPolyRS | Gifted by Prof. Peter G. Schultz | N/A |
| pMBP-LbCas12a | Chen et al., 2018 | Addgene Plasmid # 113431 |
| pET22B-AsCas12a-2C-NLS | This paper | N/A |
| pET22B-Cas12a-BE | This paper | N/A |
| pET22B-LbCas12a-2C-NLS | This paper | N/A |
| pET22B-enAsCas12a-2C-NLS | This paper | N/A |
| **Software and algorithms** | | |
| Tanon Gis | Tanon | N/A |
| CytExpert 2.3 | Beckman Coulter | https://cytexpert.software.informer.com/2.3/ |
| Gen5 | BioTek | https://www.biotek.com/products/software-robotics-software/gen5-microplate-reader-and-imager-software/ |
| GraphPad 6.01 | GraphPad | https://www.graphpad.com/dl/96314/10B92408/ |
| **Other** | | |
| Amicon® Ultra-15 Centrifugal Filter Units 50K | Millipore | Cat# UFC905024 |
| Superdex® 200 increase 10/300 GL | Cytiva | Cat# 28990944 |
| Prometheus NT.48 instrument | NanoTemper Technologies | PR-C006 |
| Tanon 1600R Gel Imaging System | Tanon | Tanon 1600R |
| NanoDrop One/OneC Microvolume UV-Vis Spectrophotometer | ThermoFisher | ND-ONE-W |
| T100 thermal cycler | Bio-Rad | 1861096 |
| Electroporator | Celetrix LLC, Manassas VA | CTX-1500A LE |
| Electroporation tube | Celetrix LLC, Manassas VA | Cat# 12-0107 |
| CellDrop Automated Cell Counters | DeNovix | N/A |
| DynaMag-5 Magnet | Invitrogen | Cat# 12303D |
| CytoFLEX LX Flow Cytometer | Beckman | N/A |
| MoFlo XDP | Beckman | N/A |
| 4D-Nucleofector | Lonza | AAF-1002B |
| Synergy H1 Hybrid Multi-Mode Reader | BioTek | Synergy H1 |

## RESOURCE AVAILABILITY

### Lead contact

Further information and requests for reagents can be directed to, and will be fulfilled, by the lead contact Tao Liu (taoliupku@pku.edu.cn).

### Materials availability

Plasmids, primers, recombinant proteins, experimental strains, and any other research reagents generated by the authors will be distributed upon request to other research investigators under a material transfer agreement.

### Data and code availability

- Any data reported in this paper will be shared by the lead contact upon request.
- This paper does not report original code.
- Any additional information required to reanalyze the data reported in this paper is available from the lead contact upon request.

## EXPERIMENTAL MODEL AND SUBJECT DETAILS

### Cell culture

HEK293, NIH/3T3, Jurkat, K562 and NALM-6 cells were purchased from American Type Culture Collection (ATCC, Manassas, VA, USA). HEK293 cells, HEK293-EGFP-TetOn(Ling et al., 2020c) reporter cell line and NIH/3T3 cells were cultured at 37°C with 5% $CO_2$ in advanced Dulbecco's Modified Eagle's Medium (MACGENE) containing 10% fetal bovine serum (PAN-Biotech). Jurkat, K562 and NALM-6 cells were cultured at 37°C with 5% $CO_2$ in RPMI-1640 (MACGENE) containing 10% fetal bovine serum (PAN-Biotech). Fresh human peripheral blood mononuclear cells were isolated from healthy donors with Ficoll-Paque PLUS (GE Healthcare). Then human T cells were purified using Dynabeads Untouched Human T Cells Kit (InvitrogenTM) and further activated with XYbeads Human CD3/CD28 T Cell Activator (Sailybio) at 1:1 ratio. T cells were cultured at 37°C with 5% $CO_2$ in X-VIVO 15 media (Lonza) with 10% inactivated fetal bovine serum (GIBCO), 30 IU/mL IL-2 (SinoBiological) 5 ng/mL IL-7 (SinoBiological) and 5 ng/mL IL-15 (SinoBiological).

## METHOD DETAILS

### General information

For all chemical synthesis, solvents and reagents were purchased from Sigma-Aldrich unless otherwise noted. Oligonucleotide synthesis and Sanger sequencing of DNA fragments or plasmids were performed by Genewiz. All the chemical modified RNA (DBCO) and synthesized RNA were purchased from General Biosystems (Anhui) Co.Ltd (Sequences were listed in Table S1). All of the polymerase chain reactions (PCR) were conducted using the 2 × Phanta Max Master Mix (Vazyme P525-01).

### Plasmid construction

All of the plasmids were constructed using Gibson assembly (New England Biolabs), and the primers used in this study are listed in Table S2. The gene of AsCas12a was amplified from the plasmid pcDNA3.1 AsCas12a, which is gifted by Prof. Du Quan from Peking University School of Pharmaceutical Science. Gene fragment of CD19-CAR was synthesized from General Biosystems (Anhui) Co.Ltd and cloning to AAV package vector. The complete sequences of Anti CD19-CAR sequence are presented in Table S3. Mutagenesis PCR was conducted using KOD-One PCR Master Mix (TOYOBO), followed by DpnI (NEB) digestion.

### Protein expression and purification

The pET-22B plasmid encoding protein coding sequence (Table S5) was transformed into the *E. coli* BL21 (DE3) strain for protein production. For mutant protein expression, pUltra-MjPolyRS was co-transformed into BL21 (DE3) strain. The protein expression and purification methods are summarized below. Briefly, cells were grown at 37°C to $OD_{600}$ of 0.6∼0.8, 0.2mM IPTG (Inalco Pharmaceuticals) and 1 mM AeF for mutant Cas12a expression were added after cooling at 4°C for 20min. Cells were grown at 18°C overnight and harvested by centrifugation at 8,000 rpm 15min at 4°C. The protein was first purified by $Ni^{2+}$ affinity chromatography. Bacteria pellets were resuspended in lysis buffer (50 mM Tris-HCl pH 8.0, 1 M KCl,10 mM imidazole), The supernatant was incubated at 4°C for 1 h with Ni-NTA agarose then transfer to a gravity column and washed with wash buffer (50 mM Tris-HCl pH 8.0, 1 M KCl, 20 mM imidazole) with 10-20 column volume. Finally, protein was eluted with elution buffer (50 mM Tris-HCl pH 8.0, 1 M KCl, 250 mM imidazole), then concentrated and changed into PBS buffer using Amicon Ultra-15 Centrifugal Filter Devices 50K (Millipore) at 5,000 g. The protein was further purified by size-exclusion chromatography (Superdex® 200 10/300 GL, Cytiva) under PBS buffer. Fractions were collected and buffer was changed to stock buffer (PBS+10% glycerol) using 50K Amicon Ultra column (Millipore). Purified protein was analyzed by SDS-polyacrylamide gel electrophoresis.

### *In vitro* transcription of crRNA

DNA templates for crRNA transcription were obtained by annealing two primer containing a T7 promoter and crRNA sequence (Sequences are listed in Table S4). Transcription reactions (20ul) were conducted under the guidance of HiScribe T7 High Yield RNA Synthesis Kit (NEB), with 1 μg of DNA template. Reactions proceeded at 37°C for 4 hours, and the crRNA was subsequently purified with RNA Clean & Concentrator-25 Kit (Zymo Research).

### Protein melting point analysis

The protein thermal stabilities of the wild-type and mutant Cas12a were detected in a fluorimetric analysis (label-free) by the Prometheus NT.48 instrument (NanoTemper Technologies GmbH). Thermal unfolding was performed in NanoDSF grade ultraviolet capillaries (NanoTemper Technologies) at a heating rate of 1°C/min in a range from 25 to 95°C. The protein melting temperature (Tm) was calculated from the first derivative of the 330 nm:350 nm ratio. Experiments on Cas12a and AzCas12a were carried out at 2 mg/mL; each sample was dialyzed into 1 × PBS, and 20 μL was loaded onto the capillaries.

### *In vitro* DNA cleavage assay

Target DNA template used for cleavage activity was PCR amplified from plasmid pcDNA3.1-EGFP. Cas12a (3pmol) with crRNA (3.6pmol) was mixed and incubated at room temperature for 10 min. Then, 150 ng of DNA template was added to pre-formed RNP complexes and incubate for 1 h at 37°C in 1 × NEB Reaction buffer. After reaction, Cas12a RNP was further heated to inactive at 65°C for 10min. The cleavage product was analyzed on 1% agarose gel. Relative intensities of full length and Cas12a-cleavage DNA fragments were determined on a Tanon 1600R Gel Imaging System.

### *In vitro* RNP assembled and electroporated in cell lines

Wild-type or mutant protein was mixed with WT/DBCO RNA at 1:1.2 molar ratio with gentle mixing at room temperature for 10 min and then incubated at 4°C for another 3 hours for chemical covalent reaction. The RNP conjugation efficiency was validated by SDS-PAGE before electroporation into cell. The electroporation machine (CTX-1500A LE), tubes (20 μl; 12-0107), and the buffer (13-0104) were provided by Celetrix LLC, Manassas VA. For electroporation, cells were harvested, washed with 1x PBS buffer, and resuspended in electroporation buffer at the density of 1 × $10^6$ cells/ 20ul reaction system. The RNP complex was mixed with the cells and transferred to a 20 μL electroporation tube. For HEK293-EGFP-TetOn reporter cells, 30pmol RNP were electroporated under the optimized condition (420V 30ms). For K562, Jurkat and NIH/3T3 cell, 30pmol RNP complex were used under the electroporation condition: 380V 30ms; 400V 30ms; 400V 30ms, respectively. After electroporation, the cells were immediately applied to pre-warmed medium for cultivation.

### EGFP disruption assay and flow cytometry analysis

Doxycycline 100X dilution (Sigma-Aldrich) was added to HEK293-EGFP-TetOn reporter cells 24 hours after electroporation. 48 hours after electroporation, cells were collected, resuspended in PBS buffer and detected by Beckman CytoFLEX Flow Cytometer. The acquired data were further analyzed using CytExpert software. In all experiments, a minimum of 10,000 cells were analyzed. Live cells were gated on the basis of forward scatter area (FSC-A) and side scatter area (SSC-A). Cells in the gate were further used to quantify the percentage of EGFP-positive populations.

### Genomic DNA purification and PCR amplification

Cells were harvested 48h after electroporation, the genomic DNA (gDNA) was then extracted and purified with a FastPure Cell/Tissue DNA Isolation Mini Kit (Vazyme) following the manufacturer's instructions. Concentrations of gDNA were determined on a NanoDrop One/OneC Microvolume UV-Vis Spectrophotometer (ThermoFisher). Genomic regions flanking the on-target sites were amplified using 500 ng of purified gDNA template, 2 × Phanta Max Master Mix (Vazyme) and specific primers on a T100 thermal cycler (Bio-Rad).

### T7E1 cleavage assay

The PCR products were re-annealed in NEB buffer 2 (50 mM NaCl, 10 mM Tris-HCl, 10 mM $MgCl_2$, 1 mM DTT, pH 7.9) (New England Biolabs) by heating to 98°C for 10 min, followed by a 2°C per cycle ramp down to 85°C, 1 min at 85°C and a 0.1°C per cycle ramp down to 25°C on a T100 thermal cycler (Bio-Rad). Subsequently, the annealed samples were digested by T7 Endonuclease I (Vazyme) for 30 min, separated by a 1% agarose gel and quantified on Tanon 1600 gel imaging system using quantity software TanonGis.

### Off-target detection by Guide-seq

WT Cas12a or cCas12a (60pmol) and dsODN (90pmol) were pre-mixed at 4 degree for 3 hours before electroporation. RNP-dsODN were electroporated into HEK293 cells by 4D-Nucleofector (Lonza). Cells were harvested approximately 3 days post transfection and genomic DNA was extracted using TIANamp Genomic DNA Kit (DP304). Library construction, Guide sequencing and data analysis was completed by GeneRulor Company Bio-X Lab, Guangzhou 510006, Guangdong, China.

### Off-target detection by Site-seq

WT Cas12a or cCas12a (90nM) RNP were pre-mixed at 4 degree for 3 hours before digestion the genomic DNA. After fragmentation, adaptor ligation, affinity purification to enrich Cas12a cleavage fragments, the fragments were amplified and added index for library construction, the final library were sequenced using NGS sequencing. Library construction, Site-seq and data analysis was completed by GeneRulor Company Bio-X Lab, Guangzhou 510006, Guangdong, China.

### Off-target detection by PEM-seq

Human DNMT1 Gene was chosen for genome editing and off-target detection (Supplementary 1). WT Cas12a or cCas12a (60pmol) were electroporated in HEK293 cell as above-mentioned methods. Procedures for preparing PEM-seq was the same as literature reported. In general, biotinylated primers was designed at 150 bp around target site to achieve primer extension. Locus specific primer was used for nested PCR. All the PEM-seq libraries were sequenced by Hiseq. Data analysis for off-target identification can follow the protocol described previously.

### HDR complex preparation and electroporation

For HDR Complex preparation, WT Cas12a RNP or cCas12a RNP and ssODN (Sequences are listed in Table S4) were mixed at 1:0.6 molar ratio before electroporation. HEK293 cells were resuspended at a density of $1 \times 10^6$ cells per reaction with electroporation buffer. The HDR Complex was mixed with cells and transferred into 20 μL electroporation tubes for electroporation. The electroporation condition for HEK293 cells was 420V for 30ms at one pulse. After electroporation, the cells were immediately transferred to prewarmed medium for cultivation. The electroporation buffer (13-0104), tube (12-0107) and electroporator (CTX-1500A LE) were provided by Celetrix LLC, Manassas VA.

### Cas12-BE RNP preparation and cell electroporation

The electroporation machine (CTX-1500A LE), tubes (20 μl; Catalog no. 12-0107), and the buffer (Catalog no. 13-0104) were provided by Celetrix LLC, Manassas VA. RNP was prepared by mixing Cas12a-BE or AzCas12a-BE protein with crRNA at 1:1.2 molar ratio at 4°C for ~3h. 293T cells were harvested, washed with 1 × PBS, and resuspended in electroporation buffer at the density of $1 \times 10^6$ cells/reaction. Then the RNP complex was mixed with the cells and transferred to a 20 μL electroporation tube. The electroporation condition was at 420 V for 30 ms at one pulse. After electroporation, the cells were immediately applied to pre-warmed DMEM medium.

### AAV production and purification

AAV CD19-CAR, pHelper plasmid, and AAV6-RC serotype plasmid together with polyethyleneimine were prepared at the ratio of 1.3:1:1, 20 μg plasmid were transfected to AAV293 with PEI in 10 cm dishes. Transfected cells were collected with PBS 72 h after transfection. AAV production, purification and tittering were operated by Vigene Biosciences.

### CAR-Jurakt / CAR-T cell preparation

Different concentrations of RNPs were prepared at a protein: RNA = 1:1.2 ratio with gentle mixing at room temperature for 5 min and then incubated at 4°C for another 3 hours. Cells were centrifuged and resuspended at a density of $1.5 \times 10^6$ cells per electroporation reaction. 20 μL Jurakt/ T cells resuspension in electroporation buffer were mixed with the prepared RNPs and transferred to electroporation tube. For Jurkat, the electroporation condition was 400V for 30ms at one pulse. After electroporation, the cells were immediately transferred back to prewarmed RPMI-1640 medium for cultivation. AAV was added into the Jurkat cells 4h after electroporation at MOI = $1 \times 10^6$. Electroporation of human primary T cells was performed 3 days after first activation. Before electroporation, XYbeads Human CD3/CD28 T Cell Activator (Sailybio) was removed with DynaMag-5 Magnet (Invitrogen). The electroporation was performed with 420V for 20ms at one pulse. After electroporation, the cells were transferred into prewarmed X-VIVO medium for cultivation. AAV was added into the T cells 4h after electroporation at MOI = $1 \times 10^6$. The electroporation machine (CTX-1500A LE), tubes (20 μl; 12-0107), and the buffer (13-0104) was provided by Celetrix LLC, Manassas VA.

### LDH-Glo cytotoxicity assay

Cytotoxic of CAR-T was evaluated with LDH-Glo Cytotoxicity Assay (Promega) following the manufacturer's instructions. NALM-6 cells were co-cultured with CAR-T cells in fresh medium as mentioned above, and 1 μL medium supernatant was diluted at 1:100 for LDH assay.

### Immunological characteristic of CAR-T cells

Five days post-electroporation, $1*10^4$ CD19-positive NALM-6 cells were seeded in a 96-well plate (NEST), and anti-CD19 CAR-T cells were added at an E/T ratio of 10:1. After co-culture for 24-48h, cells were centrifuged and supernatant was collected for immunological characteristic of T cells. An enzyme-linked immunosorbent assay was performed for detecting cytokine release of CAR-T cells using Human IFN gamma Uncoated ELISA kit (Invitrogen) and Human TNF alpha Uncoated ELISA kit (Invitrogen) following the manufacturer's instructions. The absorbance was measured by Synergy H1(BioTek).

### Semiquantitative in-and-out PCR

An in-and-out PCR approach was used for semiquantitative ratio of CAR integration at TRAC locus. Three specific primers were used for an In-Out PCR reaction, in detail, TRAC-1st-FW (CCCTTGTCCATCACTGGCAT) binds to the left homologous arm of TRAC locus, CAR-T-PCR-FW (GGAGTACGACGTGCTGGATAAG) specifically recognizes a sequence within anti-CD19 CAR fragment, TRAC-2st-RV (GCACACCCCTCATCTGACTT) binds to the right homologous arm of TRAC locus. The PCR product was analyzed by a 1% agarose gel and quantified on Tanon 1600 gel imaging system using Quantity software Tanon Gis.

### NGS sequencing

NGS primers were designed for fragment amplification, the PCR products were purified by magnetic bead and sequenced on Illumina platform. The library construction and sequencing were performed by GeneRulor Company Bio-X Lab, Guangzhou 510006, Guangdong, China, the gene editing efficiency were analyzed by CRISPResso tools.

### Multiplex gene editing in Jurkat and T cell

Wild-type or mutant Cas12a proteins (30pmol individual) were mixed with WT/DBCO crRNA targeting TRAC, β2M, PD1, CTLA4 at 1:1.2 molar ratio with gentle mixing at room temperature for 5 min and then incubated at 4°C for another 3 hours. The final RNPs were added into cells and mixed before electroporation. The electroporation condition was the same as mentioned above.

## QUANTIFICATION AND STATISTICAL ANALYSIS

### T7E1 cleavage assay quantification

The mutation frequency (indel, %) was calculated with the following formula: 100 × (1 − fraction cleaved), where fraction cleaved was defined as: density of digested products/ (density of digested products+ undigested parental products).

### EcoRI knock-in efficiency evaluation

Genomic DNA was extracted 48 hours after electroporation, and then the target region was amplified and purified. Then the PCR product was digested with 1 μL EcoRI-HF® (NEB) in CutSmart® buffer (NEB). The digested product was evaluated by electrophoresis on 1% agarose gel and analyzed by Quantity software Tanon Gis. The HDR efficiency was calculated by the following formula: %HDR efficiency = 100*density of the digested products/ (density of the digested products + undigested parental products).

### Flow cytometry analysis of CAR knock in efficiency

The CAR positive ratio of T cells and Jurkat cells was analyzed by flow cytometry 5 days after electroporation. $1 \times 10^6$ cells were incubated with c-Myc mouse monoclonal antibody (Invitrogen) at 4°C for 1h in 100 μL PBS containing 1% fetal bovine serum, and then stained with Anti-mouse IgG (H+L), $F(ab')_2$ Fragment (Alexa Fluor® 647 Conjugate) (Cell Signaling Technology) at 4°C for 30min in PBS. Stained cells were measured on CytoFlex flow cytometer (Beckman) and further analyzed using CytExpert software.

### LDH-Glo cytotoxicity quantification

The cell cytotoxicity (%) was calculated with the following formula: %cytotoxicity = 100 × (Experimental LDH Release - Medium Background)/ (Maximum LDH Release Control - Medium Background).

### Cell viability quantification

Trypan-blue stain was performed for cell viability test. Cells were mixed with 0.4% Trypan Blue Solution (GIBCO) at 1:1 volume ratio, then cell viability was determined by CellDrop Automated Cell Counters (DeVovix).

### Flow cytometry analysis of T cell for multiple gene editing

The efficiency of multiple gene editing in T cells was determined by flow cytometry 5 days after electroporation. On the 4th day after electroporation, cells were re-activated with XYbeads Human CD3/CD28 T Cell Activator (Sailybio) at 1:1 ratio. For flow cytometry, $1 \times 10^6$ cells were incubated with APC anti-human CD3 (Biolegend), FITC anti-human β2-microglobulin (Biolegend), PE anti-human CD279 (Biolegend), PE/Cyanine7 anti-human CD152 (Biolegend), or a combination of antibodies mentioned above at 4°C for 1h in 100 μL PBS containing 1% fetal bovine serum. Then the stained cells were mensured on CytoFlex flow cytometer (Beckman) and further analyzed using CytExpert software. For quadruple-negative cells sorting, $1 \times 10^7$ cells were stained in equal proportion as mentioned above, and sorted on MoFlo XDP (Beckman).

### Statistical analysis

Data were analyzed by GraphPad Prism 8. For the comparisons, Unpaired Student's t test was used. Error bars represent as standard deviation (SD) from data in at least triplicate experiments and these have stated in the corresponding legends. See Method Details and figure legends for details.

## ADDITIONAL RESOURCES

### Detailed protocol

A detailed bench protocol is available as Methods S1.